^{1}H-NMR Metabolomics Analysis of The Intervention Effects of Ruangan Xiaoji Decoction on CCl_4 Induced Liver Fibrosis in Rats

Weiliang Zhu
Zhejiang University Hospital
Guoqing Wu
Tongde Hospital of Zhejiang Province
Wenrui Zhu
Shaoxing Hospital of Traditional Chinese Medicine
Tianwen Zhao
Shaoxing Hospital of Traditional Chinese Medicine
Hong-Jiang Zhang (jian871211@sina.com)
Zhejiang Province Academy of Traditional Chinese Medicine https://orcid.org/0000-0001-8549-5425
Hongfeng Xu
Shaoxing Hospital of Traditional Chinese Medicine

Research

Keywords: liver fibrosis, Ruangan Xiaoji Decoction, 1H-NMR metabolomics, biochemical assessment

Posted Date: October 16th, 2020

DOI: https://doi.org/10.21203/rs.3.rs-90745/v1

Abstract

Background: Liver fibrosis is a common consequence of chronic liver diseases resulting from multiple etiologies. Early clinical application shows that Ruangan Xiaoji Decoction (RGXJD) has a very obvious effect on the treatment of liver fibrosis. However, the mechanism of RGXJD cures liver fibrosis requires further elucidation.

Methods: In this work, the therapeutic effect of RGXJD on CCl_4-induced liver fibroses serum and liver tissue metabolite changes in rat was analyzed by ^{1}H-NMR metabolomics. Meanwhile, histopathology examinations and serum clinical chemistry analysis verified the experimental results of metabolomics.

Results: RGXJD treatment could reverse the increase in ALT and AST induced by CCl_4 and attenuate the pathological changes in liver tissue. In the ^{1}H-NMR metabolomic analysis, PLS-DA score plots demonstrated that the serum and liver tissue metabolic profiles in rats of the RGXJD groups were similar those of the control group, yet remarkably apart from the CCl_4 group. The mechanism may be related to the endogenous metabolites including energy metabolism, amino acid metabolism, TCA cycle and purine metabolism in rats. Correlation analysis were then performed to further confirm the metabolites involved in Isoleucine, Tyrosine, UDP-Glucose, Glutathione and Leucine, etc.

Conclusions: These findings may provided new insights into the mechanism of the hepatoprotection of RGXJD.

Background

Hepatic fibrosis (HF) is a pathological feature of the liver caused by the continuous scarring reaction caused by acute or chronic injury of the liver under different metabolic, viral and chemical toxic stimuli[1]. Due to the many factors and complicated pathogenesis of liver fibrosis, although modern pharmacological research on anti-HF has been carried out for many years, some progress has been made in some animal models, and the research ideas and drug targets are also quite clear. In terms of therapeutic application, research on anti-HF drugs has not yet made major breakthroughs[2]. Recently, herbal medicines as alternative methods have attracted much interest, especially due to their superiority in treating liver fibrosis and their few side effects[3, 4].

As we know, Traditional Chinese Medicines (TCM) plays an irreplaceable role in the treatment of liver fibrosis[3, 5–7]. Based on the dialectical theory of liver fibrosis and the characteristics of qi deficiency and blood stasis, our self-made prescriptions Ruangan Xiaoji Decoction (RGXJD) composed of *Ecklonia kurome*, *Curcuma rcenyujin*, *Bupleurum chinense*, *Fritillaria thunbergii*, *Salvia miltiorrhiza*, *Hedyotis diffusa* has achieved very good curative effects in clinical treatment of liver diseases[8]. However, the exact liver protection mechanism of RGXJD in liver fibrosis was still looking forward to further elucidation. It is well known that the characteristic of herbal medicine is chemical constituent complex and multiple targets in different pathways. Understanding the mechanism of herbal medicines is

challenging[9]. Therefore, studying this overall therapeutic effect will provide a deeper understanding of the liver protective of RGXJD in the treatment of liver fibrosis.

Metabolomics is a newly developed subject after genomics, proteomics and transcriptomics. It can comprehensively assess the overview of endogenous metabolic changes in living systems and provide relevant information and valuable insights into physiological changes[10]. Metabolomics has developed rapidly in recent years and has been widely used in the field of TCM research, providing new ideas and platforms for the study of complex theoretical systems of TCM[11, 12]. Common analytical techniques in metabolomics include nuclear magnetic resonance (NMR), liquid chromatography-mass spectrometry (LC-MS), and gas chromatography-mass spectrometry (GC-MS)[13]. ^{1}H-NMR spectroscopy provides a fast, non-destructive and high-throughput method for analyzing biological fluids or tissues[14]. Recently, the combination of ^{1}H-NMR-based metabolomics with pattern recognition methods and partial least squares discriminant analysis (PLS-DA) provides an effective method for evaluating the pathological mechanism of liver fibrosis and the protective of TCM[15].

In this study, we established a rat model of CCl_4-induced liver fibrosis and used ^{1}H-NMR technology to investigate the changes in the metabolomics of liver fibrosis rats after RGXJD treatment, focusing on the metabolomics features found in pre-clinical studies. The results clarified the effect of RGXJD on the metabolomics of liver fibrosis rats and laid the foundation for elucidating the mechanism of RGXJD from the perspective of metabolomics.

Materials And Methods

Animal experiments and sample collection

A total of 40 male Sprague-Dawley rats (200 ± 20 g) were provided by the Experimental Animal Center of Zhejiang Academy of Traditional Chinese Medicine (Zhejiang, China; Certification number SYXK-Zhe 2014-0003). Rats were housed and maintained on a 12 h dark/light cycle in temperature controlled rooms (25 ± 2 ℃, 50 ± 5% humidity) with access to food and water ad libitum. Animal welfare and experimental protocols were approved by the institutional ethics committee of Zhejiang University. After 1 week, the rats were randomly divided into four groups: control group, model group, colchicine treatment group and RGXJD treatment group. The model group, RGXJD treatment group and colchicine treatment group received CCl_4 (0.1 ml/100 g body weight) and olive oil were mixed at the rate of 1:1 (v/v) to induce hepatic fibrosis. The control group received olive oil (0.1 ml/100 g body weight, i.g.) and distilled water (0.5 ml/100 g, i.g.), the model group received CCl_4 olive oil solution (0.1 ml/100 g body weight, 1:1, v/v, i.g.) and distilled water (0.5 ml/100 g, i.g.), the RGXJD treatment group received CCl_4 olive oil solution (0.1 ml/100 g body weight, 1:1, v/v, i.g.) and an i.g. dose of 2.5 g/kg body weight of RGXJD (0.5 ml/100 g), and the colchicine group received CCl_4 olive oil solution (0.1 ml/100 g body weight, 1:1, v/v, i.g.) and an i.g. dose of 0.1 mg/kg body weight of colchicine (0.5 ml/100 g). In addition, all of the groups except the control group was given an i.g dose of 0.1 ml/100 g body weight of 50% CCl_4 olive oil

solution (0.1 ml/100 g body weight, 1:1, v/v, i.g.) twice a week for six weeks. All of the drugs were administered orally once a day begun at 5 weeks after modeling.

Rats were sacrificed 24 h after the last drug administration, and blood samples were collected via the abdominal aorta after intraperitoneal injection of 10% chloral hydrate. Serum was isolated by centrifugation for 10 min at 13000 rpm at 4 ℃ (Fichal centrifuge TDL-5A, Shanghai, China) and stored at -80 ℃ for biochemical analyses. The liver was rapidly dissected, weighed and cut into small pieces and perfused with precooled saline immediately, and a part of the liver was collected in 10% buffered formalin for Sirius red staining and the remaining tissue was quickly frozen in liquid nitrogen and then stored stored at -80 ℃ until further analysis.

Sample preparation

The serum was thawed at room temperature and centrifuged at 13000 rpm at 4 ℃ for 20 min and 400 μl of the supernatant transferred to 5 mm NMR tubes and mixed with 200 μl PBS (containing TSP at 2.0 mg/ml) for analysis.

The frozen liver tissue was weighed and mixed with ACN-water (1:1, v/v) for (1:5, g/ml), and the mixture was homogenized in ice/water bath and vortexed, followed by centrifugation at 13,000 rpm for 10 min at 4 ℃. The collected supernatant was concentrated under a stream of nitrogen and then lyophilized. Dried cerebrum extracts were reconstituted in 550 μL D_2O phosphate buffer [0.2 M Na_2HPO_4 and 0.2 M NaH_2PO_4, pH 7.4, containing 0.05% TSP]. The residues were removed by vortexing and centrifugation at 13,000 rpm for 10 min at 4 °C, and the transparent supernatant solution was transferred into 5-mm NMR tube for NMR analysis.

Acquisition of ^{1}H NMR data

^{1}H-NMR spectra were recorded on a Bruker AVANCE 600 MHz spectrometer (Bruker GmbH, Karlsruhe, Germany) at 25 ℃. 1H NMR spectra were collected with 128 transients into 32,768 (32 K) data points over a spectral width of 10,000 Hz, with an acquisition time of 3.27 s and a relaxation delay of 3.0 s. The free induction decays (FIDs) were determined by an exponential window function with a line-broadening factor of 0.3 Hz prior to Fourier transformation.

Data processing of NMR spectra

All spectra were manually phased and baseline-corrected using MestReNova software (version 6.0.2, Mestrelab Research, Santiago de Compostela, Spain). Each spectrum was segmented at 0.01 ppm intervals across the chemical shifts δ 0.6-9.0, and the chemical shift of serum and urine was referenced to the lactate at δ 1.33 and the TPS at δ 0.00. With the removal of signals of water and it's affected neighboring regions (4.30-9.00 for serum; 4.50–5.30 for liver extract) and export these spectra to ASCII files. Normalization to a total sum of all integrals for tissue extracts was conducted before multivariate analysis. Metabolites were assigned by querying publicly accessible metabolomics databases such as Human Metabolome Database (HMDB, http://www.hmdb.ca), Madison-Qingdao Metabolomics

Consortium Database (MMCD, http://mmcd.nmrfam.wisc.edu), and Kyoto Encyclopedia of Genes and Genomes (KEGG) (http://www.genome.ad.jp/kegg/).

Multivariate data analysis

Then, the resultant data in ".txt" format was imported into SIMCA-P 13.0 (version 13.0, UmetricsAB, Sweden) for multivariate statistical analysis. PCA was first performed on mean-centered data to identify outliers between the control and CY groups. PLS-DA was applied to discriminate metabolic profiles between samples groups. Orthogonal-projection to latent structure-discriminate analysis (OPLS-DA) is a supervised method to identify metabolites that contributing to the group separation. The validity of the models was assessed by 200 permutation tests, 7-fold cross-validation and CV-ANOVA method. Relative amounts of metabolites were calculated on the basis of the integrated regions (buckets) from the least overlapping NMR signals of metabolites.

In addition, the corresponding loading plots were assessed by the absolute value of the correlation coefficient, which was used to identify the metabolites that mostly contributed to the discrimination between two groups at the three-time points. The loading plots were analyzed using MATLAB software (R2016a, MathWorks Inc., Natick, MA, USA).

Experimental values were expressed as mean standard deviation (SD). Results of body weight, ALT and AST, and the peak areas (buckets) of the differential metabolites were further compared by t-test using SPSS16.0 software (SPSS Inc., Chicago, IL), and p-values less than 0.05 were considered to be significant. The comprehensive metabolic network was mapped by integration of all potential biomarkers identified in the present research by means of the KEGG and MetaboAnalyst 4.0 (http://www.metaboanalyst.ca/).

Results

Changes in animal characteristics and histopathological observations

The body weight of the rats in the CCl_4 group was lower than that in the control group after medication administration (Fig. 1). The decreases of body weights of colchicine and RGXJD groups were much greater than that of CCl_4 group. At the end of the experiment, absolute and relative liver weights were measured, which were significantly increased in CCl_4 intoxicated rats as compared with those in control rats. Meanwhile, these animal characteristics were improved by colchicine and RGXJD groups.

The biochemical characteristics demonstrated that RGXJD could effectively reduce the CCl_4 caused injury in rats (Fig. 2A-D). The elevated level of alanine transaminase (ALT) and aspartate aminotransferase (AST) in the CCl_4 group indicated that the liver was damaged, releasing ALT and AST into the blood. However, after treatment with colchicine or RGXJD, the activities of ALT, AST were significantly decreased compared with the model group, which indicated that RGXJD has positive effects on CCl_4-induced liver fibrosis in rats, and possess potent hepatoprotection.

Histopathological examination revealed the changes of clinical chemistry parameters (Fig. 2E-H). Severe changes in liver morphology were observed in the model group after administration of CCl_4, including fiber interval formation, fatty steatosis, and infiltration of inflammatory cells in the portal area, and most rat livers appeared to have pseudo lobules, which demonstrated liver fibrosis was successful established. By contrast, no apparent change was observed in the liver of control rats. Small circular vacuoles indicating slight hepatic steatosis were observed in the liver of RGXJD groups. Furthermore, the colchicine treatment group also displayed similar protective effects.

^{1}H-NMR analysis and metabolic profiling in serum and liver

The representative ^{1}H-NMR spectra of serum and liver tissue samples obtained from all groups were shown in Figs. 3 and 4. The assignments of endogenous metabolite assignments were chemical shifts reported in previous literature.

They reveal different metabolic profiles between the control and treated groups. In total, 19 and 32 metabolites were identified and quantified in serum (Fig. 3) and in liver tissue (Fig. 4), respectively.

The unsupervised principal component analysis (PCA) and supervised PLS-DA models were reconstructed to determine the metabolic changes and to characterize the metabolite profile of the control and RGXJD treated samples. The control and model groups had significant differences in PLS-DA analysis of serum and liver spectrometry, indicating that the metabolic profile changes after liver fibrosis, which are induced by CCl_4, while the colchicine and RGXJD ones appeared close to the control group. The OPLS-DA scores plots showed apparent separation between treated groups and control group, with a satisfactory goodness of fit and predictability. At the same time, we observed that there is no difference between the RGXJD and control groups. The corresponding loadings plot combined with the VIP values (VIP > 1.0) from the pattern recognition model, screened out potential biomarkers for the differentiation of colchicine, RGXJD and CCl_4 groups. Alternation of potential biomarkers was evaluated by Student's t test, and the statistical significance was accepted if $p < 0.05$. The 1H-NMR detected relative integral levels of metabolites indicating differences between all groups are listed in Tables S1 and S2.

For the serum, the coefficient-coded loadings plot (Fig. 5) and Table S1 showed the relevant changes in the endogenous metabolites responsible for the separation comparison of treated groups and control. In addition, the coefficient-coded loadings plot of RGXJD group compared with the model group, the levels of isoleucine, glycine, methanol, alanine increased obviously and had decreased in uridine levels.

For the liver, the coefficient-coded loadings plot (Fig. 6) and Table S2 showed the relevant changes in the endogenous metabolites responsible for the separation comparison of treated groups and control. In addition, the coefficient-coded loadings plot of RGXJD group compared with the model group, the levels of NAD+, xanthine, tyrosine, fumare, inosine, isoleucine, UDP-Glucose, betaine, sarcosine, glutathione, dimethylamine, lactate, leucine increased obviously and had decreased in uridine and valine levels.

Metabolic pathways analysis

In addition, we performed the metabolic pathway analysis of the integrated 27 differential metabolites. Through the MetaboAnalyst 4.0 (www.metaboanalyst.ca) topology analysis, we found that RGXJD exposure disturbed 26 metabolic pathways (Fig. 7). The correlation network was constructed by searching through the Kyoto Encyclopedia of Genes and Genomes KEGG (http://www.kegg.jp) pathway database. In the present study, our results illustrated that the comprehensive metabolic profile changes triggered by CCl_4-induced liver injured rats were largely linked to amino acid, purine metabolism, and energy metabolism, and the associated metabolic pathways of each substance are summarized in Fig. 8.

The Metabolic Pathway Analysis in Serum Samples

The 11 metabolic differences were observed in serum, which were Alanine, citrate, citric acid, glycine, inosine, lysine, methanol, uridine, 3-hydroxy butyrate and isoleucine (Fig. 7A). There was 1 metabolic pathways affected (impact > 0.1 and $p < 0.05$), Glyoxylate and dicarboxylate metabolism.

The Metabolic Pathway Analysis in Liver Samples

The 21 metabolic differences in liver were alanine, glycerin, inosine, inositol, leucine, N-acetyl glycoprotein, phenylalanine, serine, tyrosine, valine, betaine, dimethylamine, fumarate, glutathione, isoleucine, lactate, NAD+, sarcosine, UDP-glucose, uridine and xanthine (Fig. 7B). There were 4 metabolic pathways affected (impact > 0.1 and $p < 0.05$), including Aminoacyl-tRNA biosynthesis, Phenylalanine, tyrosine and tryptophan biosynthesis, Glycine, serine and threonine metabolism and Phenylalanine metabolism.

Discussion

The liver is a multifunctional organ that participates in various enzyme metabolism activities. Therefore, the damage of hepatotoxic agents to this vital organ will lead to metabolic disorders of the body[16]. CCl_4 is a classic chemical hepatotoxic agent. The rat liver injury model induced by intraperitoneal injection of CCl_4 has good reproducibility, which can cause substantial damage to liver cells and abnormal liver function[17]. The formation of free radicals and the chain peroxidation reaction caused by CCl_4 are the main mechanism of liver damage caused by CCl_4. Liver cells are attacked by free radicals, and the permeability of the cell membrane increases, leading to the release of intracellular enzymes and increasing serum enzymes[18]. This experiment replicated the acute liver injury model of SD rats induced by CCl_4. AST and ALT existed in hepatocytes. When the above indicators in the serum increase, it indicates liver injury. Compared with the normal group, the AST and ALT levels in the serum of the model group were higher, while the colchicine and RGXJD lowered the enzyme and protected the liver, and could effectively reduce the CCl_4-induced liver injury and fibrotic scar formation in rats. In this work, the ^{1}H-NMR based metabolomics method combined with histopathological measurement and biochemical parameter measurement was used to study the protective effect of RGXJD on CCl_4-induced liver fibrosis in rats. The analysis found that compared with colchicine, RGXJD has more abundant action pathways. It can protect rats from liver damage induced by CCl_4 through antioxidant, energy supply and disordered amino acid

and nucleic acid metabolism. A schematic diagram of the blocked metabolic pathway is drawn, showing the correlation of the identified metabolites.

Oxidative stress

Oxidative stress is the main mechanism of the pathogenesis of CCl_4-induced liver fibrosis in rats. Glutathione is a major antioxidant that can resist oxidative stress and protect macromolecules and cell membranes from free radical damage with the help of glutathione reductase. Glutathione levels in rats with liver fibrosis were significantly increased. The increase in glutathione levels in the model group can help organisms scavenge free radicals generated by CCl_4, thereby protecting themselves against oxidative stress. RGXJD treatment may further increase glutathione levels, indicating its ability to prevent oxidative damage.

Amino acid metabolism

Alanine is significantly increased in the liver of fibrotic rats from model group. As a component of the glucose-alanine cycle, alanine plays an important role in intermolecular nitrogen transport. The latter transports waste nitrogen from skeletal muscle to the liver and metabolizes it into urea[19]. At the same time, alanine can be used as a glycogen amino acid. Blood alanine can be transported to the liver through the glucose-alanine cycle to produce pyruvate, which is the carbon source for gluconeogenesis[20]. Because CCl_4 exposure caused severe liver damage in rats, the gluconeogenesis was inhibited, the glucose-alanine cycle was impaired, and alanine accumulated. RGXJD can effectively reduce the increase in alanine level, suggesting that RGXJD can restore the metabolism of glucose and alanine and play a role in liver protection.

Valine, leucine and isoleucine are three important essential amino acids in the body. They are important precursors and regulators of protein synthesis and collectively referred to as Branched Chain Amino Acids (BCAAs)[21]. Studies have shown that patients with liver disease are prone to hyperinsulinemia due to impaired liver function, resulting in a decrease in BCAAs in the plasma[22, 23]. Therefore, such as valine are commonly used in clinical treatment of liver failure and other liver damage caused by other factors[24]. On the other hand, valine also helps to remove excess nitrogen from the liver and transports the body's demand for nitrogen to all parts of the body[25]. At the same time, the reduction of leucine content is not conducive to stimulating the production of hepatocyte growth factor, and reduces the ability to inhibit the production of reactive oxygen species[26]. Arginine is an intermediate product of the urea cycle, a substrate of protein synthesis and a precursor of NO. The reduction of arginine content is not conducive to the protection of the liver[27]. In the model group, BCAAs in liver tissues decreased to varying degrees, which may be due to their over-utilization to repair damaged proteins in liver tissues to alleviate liver damage caused by CCL_4, while BCAAs increased significantly, which is the body’s self-protection A manifestation of the mechanism is to mobilize more BCAAs to repair the liver and fight liver damage. The BCAAs in the liver tissue of the RGXJD group continued to decline, indicating that it can speed up the liver to use BCAAs to repair damaged proteins.

Through transamination, amino acids are absorbed in the muscle in the form of glutamic acid, and then glutamic acid is transferred to pyruvate through the action of alanine aminotransferase to form alanine. It is reported in the literature that in mammals, alanine is a key intermediate in the alanine-glucose cycle[20]. After alanine is transported from the blood to the liver, it is converted into glucose through the gluconeogenesis pathway as a glycogenic amino acid in the liver, and the other part is converted for glutamic acid, ammonia is excreted in a non-toxic form through the urea cycle[28]. Alanine-glucose cycle is the physiological pathway for muscle tissue to supply energy and excrete ammonia[29]. The alanine in the blood and tissues of the model group was significantly increased, indicating that the circulation was obstructed and the liver function was impaired, resulting in accumulation of alanine that could not be effectively used.

After RGXJD intervention, the accumulation of alanine in the liver tissue was relieved to a certain extent, indicating that liver function was restored, alanine catabolism was accelerated, and alanine glucose was strengthened in the liver, and the alanine in the serum was further significant. The improvement also stimulates the improvement of the body's self-protection ability, accelerates the synthesis and supply of precursors, is used for the alanine glucose cycle, and restores the alanine glucose mechanism.

RGXJD can adjust the levels of BCAAs, alanine, etc., according to the body's self-adaptation requirements, promote glutamine to accelerate the process of glutathione synthesis, and regulate the development of amino acid metabolism in a direction beneficial to disease recovery. This may be a mechanism of its liver protection.

In addition, phenylalanine is one of the essential amino acids for the human body, and most of it is oxidized to tyrosine by phenylalanine hydroxylase in the body[30]. Tyrosine is both a sugar-producing amino acid and a ketogenic amino acid. A decrease in phenylalanine and tyrosine content indicates a decrease in gluconeogenesis in the liver and a disorder of fatty acid synthesis[31]. As the results, colchicine can adjust the level of phenylalanine in the body, but there is no significant difference in this amino acid in the RGXJD group.

Nucleic acid metabolism

The level of inosine in the liver of the model group was significantly reduced. CCl_4 and its metabolites may damage DNA directly or indirectly by stimulating the production of reactive oxygen species, and induce genetic toxicity and DNA oxidative damage in rats[32]. In purine catabolism, inosine can be catalyzed to hypoxanthine, which can then be catalyzed to xanthine by xanthine oxidoreductase[33]. Xanthine can be oxidized to uric acid, and uric acid is an effective antioxidant and free radical scavenger in the body[34]. In the model group, inosine, xanthine, hypoxanthine, and nicotinamide decreased significantly, indicating that purine metabolism was inhibited and impaired; after administration of RGXJD, it was reversed, indicating that RGXJD can restore disordered purine metabolism. RGXJD can restore the disordered purine metabolism according to the body's self-adaptation requirements, promote glutamine to accelerate the process of glutathione synthesis, promote the increase of inosine and xanthine levels, and play an anti-oxidation and anti-liver fibrosis effect.

Energy metabolism

Under normal conditions of the body, glucose is oxidized into the tricarboxylic acid cycle (TCA) under aerobic conditions to produce a large amount of energy, which is the main energy supply pathway in the body[35]. Pyruvate is the product of the second stage of glycolysis. It enters the inner mitochondrial membrane under aerobic conditions, oxidizes and decarboxylates under the action of the pyruvate dehydrogenase system to generate acetyl-CoA, which enters the tricarboxylic acid cycle [36]. Compared with the control group, the fumarate and NADPH levels of the model group were significantly reduced. Fumarate, succinate and NADPH are intermediates in the TCA cycle and/or respiratory chain. Their dysregulation in rats with liver fibrosis indicates that the TCA circulation and energy metabolism in the liver mitochondria are impaired.

In addition, a significant decrease in 3-hydroxybutyrate levels was observed in the liver of rats administered with CCl_4. As a ketone body, 3-hydroxybutyrate has been proven to be an alternative energy source, which may help the organism in the event of insufficient glucose supply and energy crisis. CCl_4 injection causes severe oxidative damage to liver cells and liver mitochondria, resulting in decreased glucose metabolism, insufficient ATP production, and decreased 3-hydroxybutyrate production. RGXJD intervention significantly increased UDP-glucose levels and restored fumarate, NADPH and 3-hydroxybutyrate diseases to a normal state, indicating that RGXJD can prevent CCl_4 from regulating fibrotic energy metabolism and repair disordered TCA cycles and inhibit glycogen deposition, thereby causing fibrosis.

In short, the mechanism of CCl_4-induced rat liver injury model is mainly related to amino acid metabolism, energy metabolism and nucleic acid metabolism. Through the mechanism of CCl_4-induced liver injury in rats, we preliminarily inferred the role of RGXJD in the treatment of liver injury. After RGXJD treatment, 19 biomarkers in rats showed a trend of improvement. These biomarkers are involved in amino acid metabolism and lipid metabolism, and most of them are amino acids. It can be inferred that RGXJD mainly treats liver damage by improving amino acid metabolism disorders. However, due to the limitations of non-targeted metabolomics testing, further studies are needed to verify the current conclusions.

Conclusions

The present study utilized a serum and liver metabolomics approach, combined with serum biochemical and histopathological tests, to investigate the hepatoprotective effect of RGXJD on the CCl_4-induced liver injury. Significant changes were found in both ^{1}H-NMR serum and liver metabolic profiles. Eighteen biomarkers related to the hepatoprotective effects of RGXJD against CCl_4-induced liver injury were discovered. Comprehensive studies demonstrated that hepatic injury, to a certain extent, could be resolved or regressed by RGXJD through partially regulating the perturbed metabolic pathways of oxidative stress, amino acid, nucleic acid and energy metabolism. Our study provided new insights into the mechanism of the hepatoprotection of RGXJD. This work also proved that comprehensive

metabolomics analysis could greatly facilitate and provide useful evidence to further comprehensively understand the mechanism of action for TCM. Moreover, the quantitative analysis of biomarkers should be done in a further study to characterize the effects of traditional Chinese medicine to prevent liver injury and protect the liver.

Abbreviations

RGXJD
Ruangan Xiaoji Decoction; HF:Hepatic fibrosis; TCM:Traditional Chinese Medicines; NMR:nuclear magnetic resonance; LC-MS:liquid chromatography-mass spectrometry; GC-MS:gas chromatography-mass spectrometry; PLS-DA:partial least squares discriminant analysis; FIDs:free induction decays; HMDB:Human Metabolome Database; MMCD:Madison-Qingdao Metabolomics Consortium Database; KEGG:Kyoto Encyclopedia of Genes and Genomes; OPLS-DA:Orthogonal-projection to latent structure-discriminate analysis; SD:standard deviation; ALT:alanine transaminase; AST:aspartate aminotransferase; PCA:principal component analysis; BCAAs:Branched Chain Amino Acids.

Declarations

Author Contributions

Conceptualization, H.Z. and H.X.; performed the experiments, W.Z. and G.W.; data analysis, W.Z. and T.Z.; writing, W.Z., H.Z. and H.X.. All authors have read and agreed to the published version of the manuscript.

Competing interests

The authors declare that they have no competing interests.

Availability of data and materials

The datasets used during the current study are available from the corresponding author on reasonable request.

Consent for publication

All authors have provided consent for publication in the Journal of Chinese Medicine.

Ethics approval and consent to participate

Animal care and experimental procedures used in the current study were approved by the Institutional Animal Care and Use Committee of Zhejiang Province Academy of Traditional Chinese Medicine (Ethics No. XMSC 2018054).

Funding

This research was supported by the Public Projects of Zhejiang Province (No. LQY19H280001) and the Science and Technology Project of Shaoxing (No. 2018C30120).

References

1. Chang ML, Yang SS. Metabolic Signature of Hepatic Fibrosis: From Individual Pathways to Systems Biology. Cells. **2019;** 8 (11): 1423.
2. Lambrecht J, van Grunsven LA, Tacke F. Current and emerging pharmacotherapeutic interventions for the treatment of liver fibrosis. *Expert Opinion on Pharmacotherapy.***2020;** 21(13): 1637-1650.
3. Li H. Advances in anti hepatic fibrotic therapy with Traditional Chinese Medicine herbal formula. *Journal of Ethnopharmacology.***2020;** 251: 112442.
4. Latief U, Ahmad R. Herbal remedies for liver fibrosis: A review on the mode of action of fifty herbs. *Journal of traditional and complementary medicine.***2018;** 8(3): 352-360.
5. Cai FF, Bian YQ, Wu R, Sun Y, Chen XL, Yang MD, Zhang QR, Hu Y, Sun MY, Su SB. Yinchenhao decoction suppresses rat liver fibrosis involved in an apoptosis regulation mechanism based on network pharmacology and transcriptomic analysis. *Biomedicine & Pharmacotherapy.***2019;** 114: 108863.
6. Zhao CQ, Zhou Y, Ping J, Xu LM. Traditional Chinese medicine for treatment of liver diseases: progress, challenges and opportunities. *Journal of Integrative Medicine.***2014;** 12(5): 401-408.
7. Hong M, Li S, Tan HY, Cheung F, Wang N, Huang J, Feng Y. A network-based pharmacology study of the herb-induced liver injury potential of traditional hepatoprotective Chinese herbal medicines. *Molecules.***2017;** 22(4): 632.
8. Zheng C. Examples of Treating Liver Diseases with Ruangan Xiaoji Decoction. *Journal of Zhejiang College of TCM.***1993;** 17 (4): 18.
9. Lin AX, Chan G, Hu Y. Ouyang, D.; Ung, C. O. L.; Shi, L.; Hu, H., Internationalization of traditional Chinese medicine: current international market, internationalization challenges and prospective suggestions. *J Chinese medicine.***2018;** 13(1): 1-6.
10. Segers K, Declerck S, Mangelings D, Heyden YV, Eeckhaut AV. Analytical techniques for metabolomic studies: a review. *Bioanalysis.***2019;** 11(24): 2297-2318.
11. Wang M, Chen L, Liu D, Chen H, Tang DD, Zhao YY. Metabolomics highlights pharmacological bioactivity and biochemical mechanism of traditional Chinese medicine. *Chemico-Biological Interactions.***2017;** 273: 133-141.
12. Song Q, Zhang AH, Yan GL, Liu L, Wang XJ. Technological advances in current metabolomics and its application in tradition Chinese medicine. *RSC advances.***2017;** 7(84): 53516-53524.
13. Zhang A, Sun H, Wang P, Han Y, Wang X. Modern analytical techniques in metabolomics analysis. *Analyst.***2012;** 137(2): 293-300.
14. Li X, Luo H, Huang T, Xu L, Shi X, Hu K. Statistically correlating NMR spectra and LC-MS data to facilitate the identification of individual metabolites in metabolomics mixtures. *Analytical and*

*bioanalytical chemistry.***2019;** 411(7): 1301-1309.

15. Liu X, Lv M, Wang Y, Zhao D, Zhao S, Li S, Qin X. Deciphering the compatibility rule of Traditional Chinese Medicine prescription based on NMR metabolomics: A case study of Xiaoyaosan. *Journal of Ethnopharmacology.***2020;** 112726.
16. Pan X, Zhou J, Chen Y, Xie X, Rao C, Liang J, Zhang Y, Peng C. Classification, hepatotoxic mechanisms, and targets of the risk ingredients in traditional Chinese medicine-induced liver injury. *Toxicology Letters.***2020;** 323: 48-56.
17. Dong S, Chen QL, Song YN, Sun Y, Wei B, Li XY, Hu YY, Liu P, Su SB. Mechanisms of CCl4-induced liver fibrosis with combined transcriptomic and proteomic analysis. *The Journal of toxicological sciences.***2016;** 41(4): 561-572.
18. Brol MJ, Rösch F, Schierwagen R, Magdaleno F, Uschner FE, Manekeller S, Queck A, Schwarzkopf K, Odenthal M, Drebber U. Combination of CCl4 with alcoholic and metabolic injuries mimics human liver fibrosis. *American Journal of Physiology-Gastrointestinal and Liver Physiology.***2019;** 317(2): G182-G194.
19. Matsumoto S, Häberle J, Kido J, Mitsubuchi H, Endo F, Nakamura K. Urea cycle disorders—update. *Journal of human genetics.***2019;** 64(9): 833-847.
20. Felig P, Wahren J. Interrelationship between amino acid and carbohydrate metabolism during exercise: the glucose alanine-cycle. In *Muscle Metabolism during exercise*, Springer: 1971; pp 205-214.
21. Zhang S, Zeng X, Ren M, Mao X, Qiao S. Novel metabolic and physiological functions of branched chain amino acids: a review. *Journal of animal science and biotechnology.***2017;** 8(1): 10.
22. Park JG, Tak WY, Park SY, Kweon YO, Jang SY, Lee YR, Bae SH, Jang JY, Kim DY, Lee JS. Effects of branched-chain amino acids (BCAAs) on the progression of advanced liver disease: a Korean nationwide, multicenter, retrospective, observational, cohort study. *Medicine.***2017;** 96(24).
23. Tajiri K, Shimizu Y. Branched-chain amino acids in liver diseases. *Translational gastroenterology hepatology.***2018;** 3.
24. Grüngreiff K, Kleine F, Musil H, Diete U, Franke D, Klauck S, Päge I, Kleine S, Lössner B, Pfeiffer K. Valine and branched-chain amino acids in the treatment of hepatic encephalopathy. *Zeitschrift fur Gastroenterologie.***1993;** 31(4): 235-241.
25. Nakagawa I, Takahashi T, Suzuki T, Kobayashi K. Amino acid requirements of children: minimal needs of threonine, valine and phenylalanine based on nitrogen balance method. *Journal of Nutrition.***1962;** 77: 61-68.
26. Iozzo RV, Schaefer L. Proteoglycans in health and disease: novel regulatory signaling mechanisms evoked by the small leucine-rich proteoglycans. *The FEBS journa.l* **2010;** 277, (19), 3864-3875.
27. Featherston W, Rogers Q, Freedland R. Relative importance of kidney and liver in synthesis of arginine by the rat. *American Journal of Physiology-Legacy Content.***1973;** 224(1): 127-129.
28. Snell K. Alanine as a gluconeogenic carrier. *Trends in biochemical sciences.***1979;** 4(6): 124-128.

29. Visek WJ. Ammonia metabolism, urea cycle capacity and their biochemical assessment. *Nutrition Reviews (USA).***1979**.
30. Lerner AB. Metabolism of phenylalanine and tyrosine. *Advances in Enzymology.***2009;** 14: 73-128.
31. Kopple JD. Phenylalanine and tyrosine metabolism in chronic kidney failure. *The Journal of nutrition.***2007;** 137(6): 1586S-1590S.
32. Kadiiska M, Gladen B, Baird D, Germolec D, Graham L, Parker C, Nyska A, Wachsman J, Ames B, Basu S. Biomarkers of oxidative stress study II: are oxidation products of lipids, proteins, and DNA markers of CCl4 poisoning? *Free Radical Biology and Medicine.***2005;** 38(6): 698-710.
33. Villalobos-García D, Hernández-Muñoz R. Catalase increases ethanol oxidation through the purine catabolism in rat liver. *J Biochemical Pharmacology.***2017;** 137: 107-112.
34. Cantu-Medellin N, Kelley EE. Xanthine oxidoreductase-catalyzed reduction of nitrite to nitric oxide: insights regarding where, when and how. *Nitric Oxide.***2013;** 34: 19-26.
35. Ying M, Guo C, Hu X. The quantitative relationship between isotopic and net contributions of lactate and glucose to the tricarboxylic acid (TCA) cycle. *Journal of Biological Chemistry.***2019;** 294(24): 9615-9630.
36. Golias T, Kery M, Radenkovic S, Papandreou I. Microenvironmental control of glucose metabolism in tumors by regulation of pyruvate dehydrogenase. *International journal of cancer.***2019;** 144(4): 674-686.

Figures

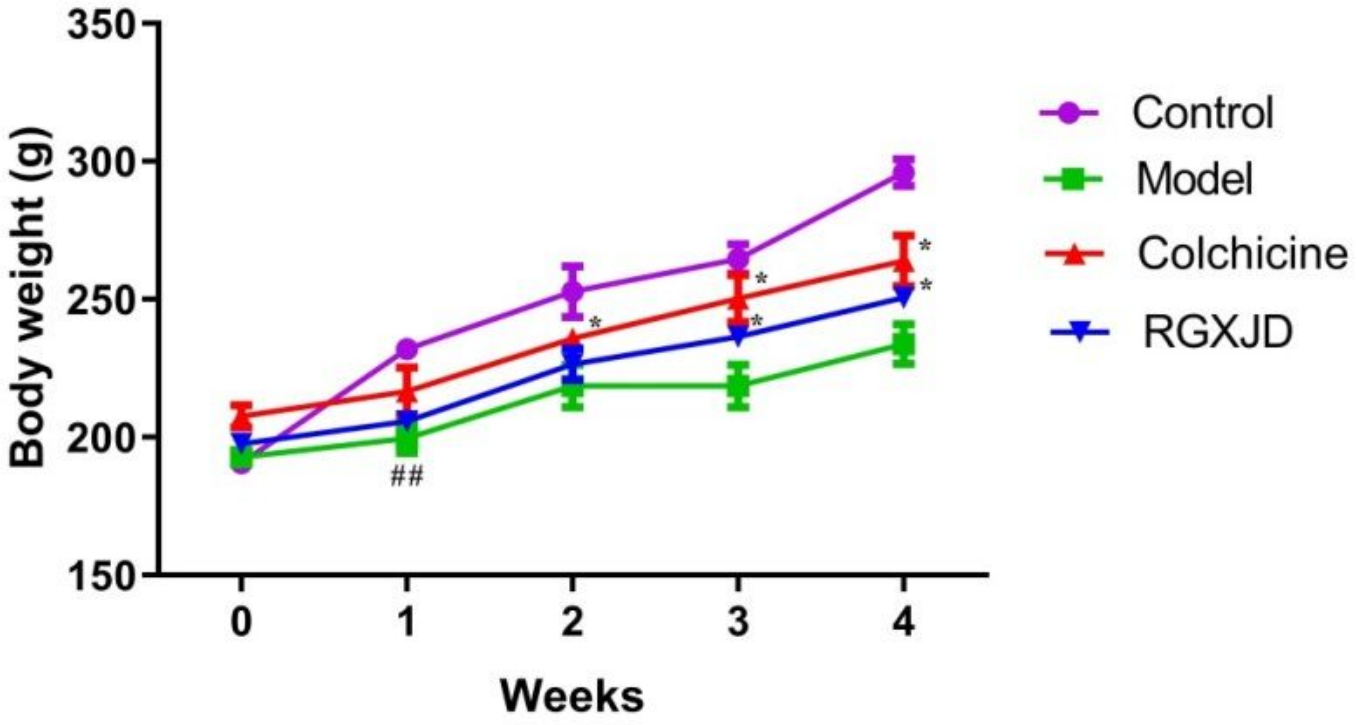

Figure 1

Effects of CCl4 on body weight from control, model, colchicine and RGXJD groups. All the values were shown as mean±SD. ##p<0.01 vs control group, *p<0.05 vs model group.

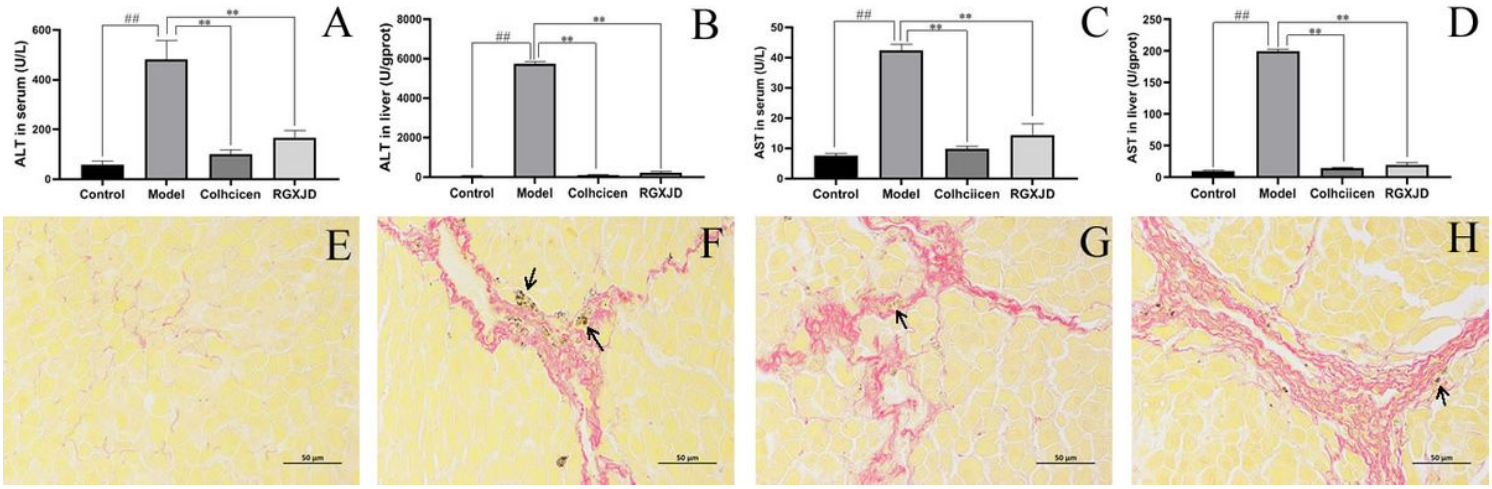

Figure 2

Biochemical assay levels of ALT and AST from serum (A, C) and liver tissue (B, D); Histological investigations of liver (E-H) show representative photomicrographs of liver sections stained with Sirius red in respective group (400 ×), E: control group, F: model group, G: colchicine treated group, H: RGXJD treated group. Compared with control, ##p<0.01, compared with model, **p<0.01.

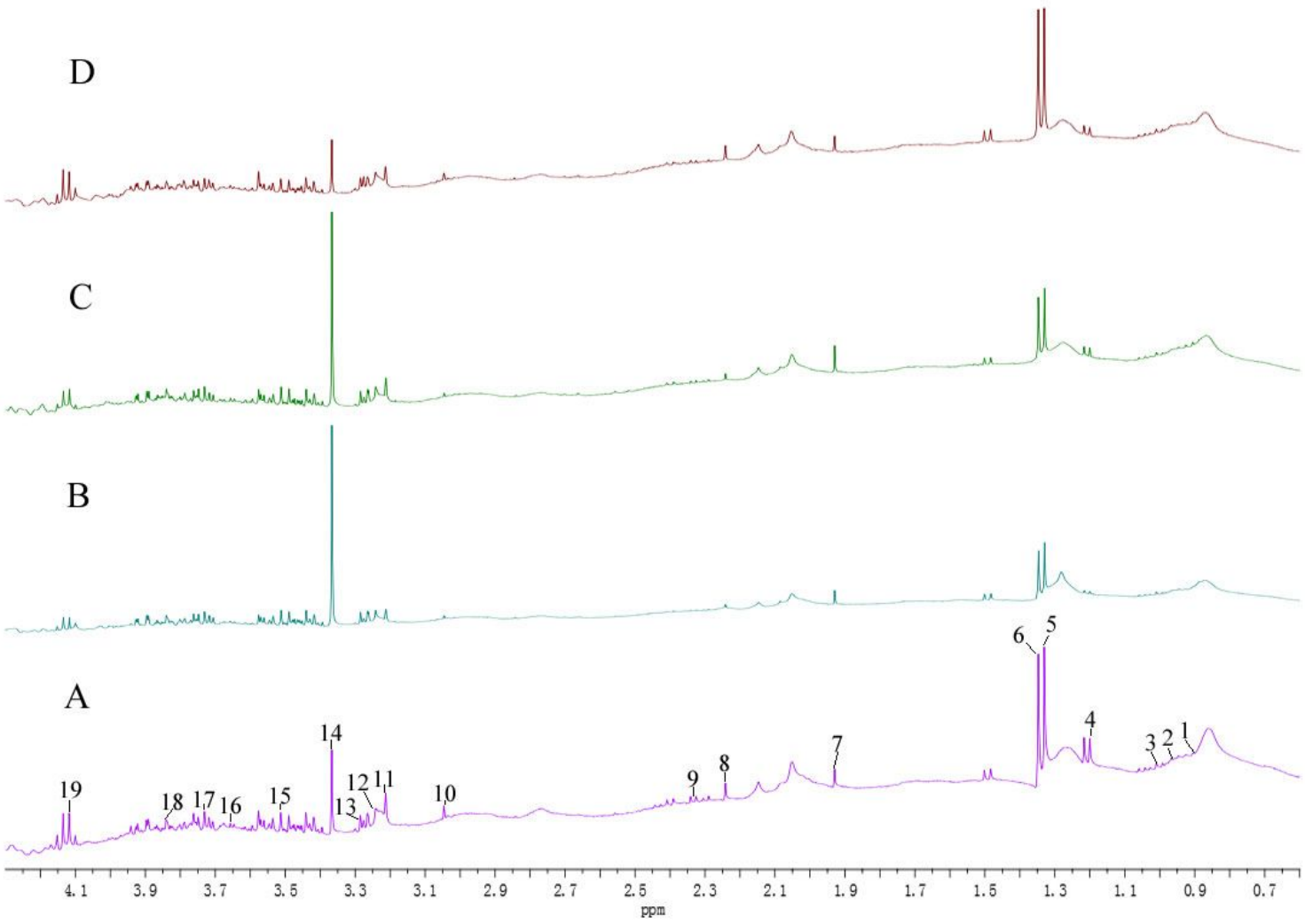

Figure 3

600 MHz spectra of serum obtained from rats from the control (A); model (B); cohcolie (C) and RGXJD (D) groups, respectively. Keys: 1, Glutamine; 2, Leucine; 3, Valine; 4, 3-Hydroxybutyrate; 5, Lactate; 6, Tryptophan; 7, Acetoacetate; 8, Acetone; 9, Pyruvate; 10, Tyrosine; 11, Phenylalanine; 12, Alanine; 13, Citrate; 14, Methanol; 15, Glycine; 16, Isoleucine; 17, Lysine; 18, Uridine; 19, Inosine.

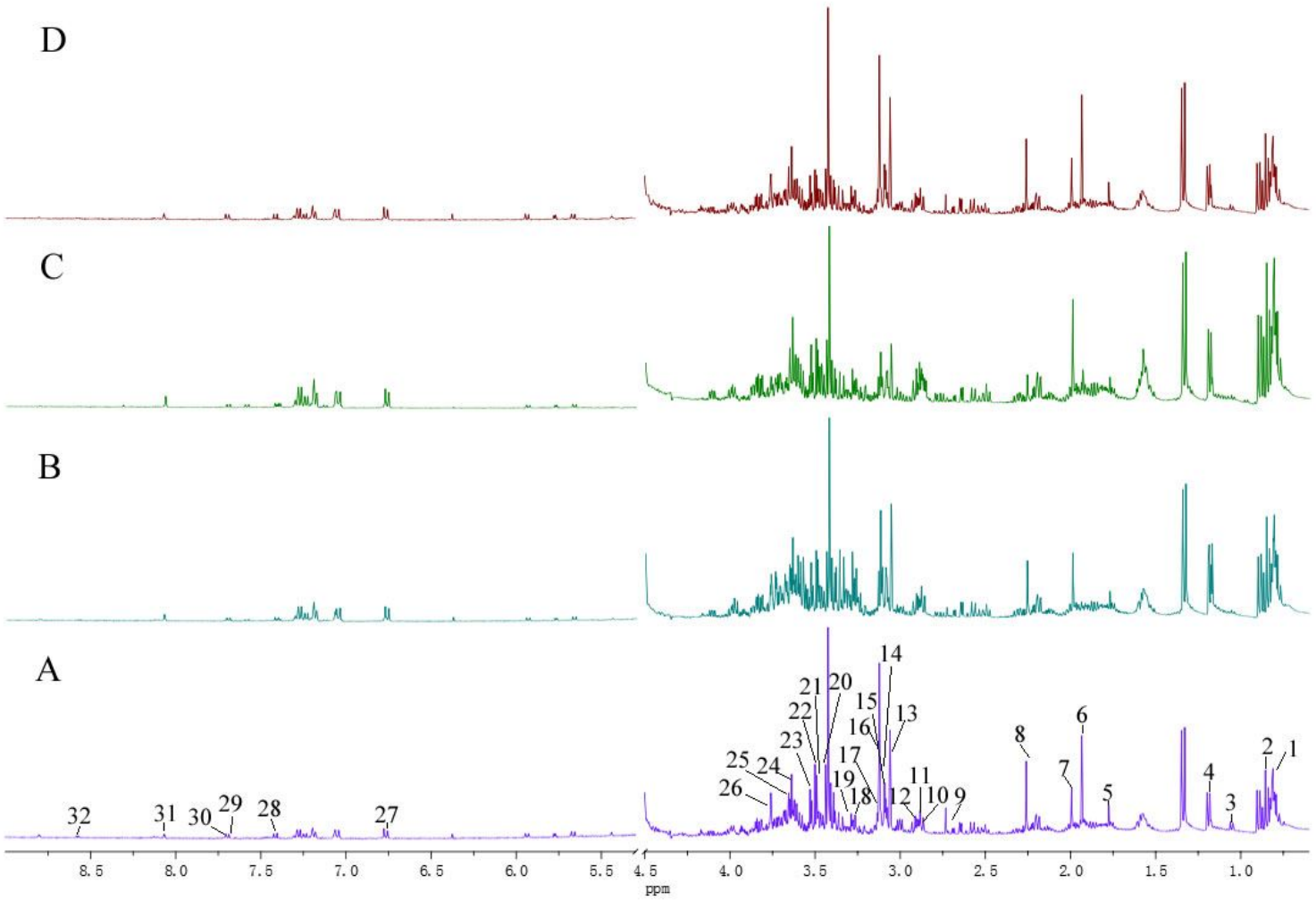

Figure 4

600 MHz spectra of liver obtained from rats from the control (A); model (B); cohcolie (C) and RGXJD (D) groups, respectively. Keys: 1, Leucine; 2, Valine; 3, 3-Hydroxybutyrate; 4, Lactate; 5, Dimethylamine; 6, Glutamate; 7, Glutathione; 8, Glutamine; 9, 5,6-Dihydrouracil; 10, NADPH; 11, Sarcosine; 12, Aspartate; 13, Creatine; 14, Tyrosine; 15, Phenylalanine; 16, Histidine; 17, Choline; 18, Phosphoethanolamine; 19, sn-Glycero-3-phosphocholine; 20, UDP-glucose; 21, Betaine; 22, UDP-galactose; 23, Glycine; 24, Isoleucine; 25, Lysine; 26, Uridine; 27, Inosine; 28, Fumarate; 29, Niacinamide; 30, Xanthine; 31, Hypoxanthine; 32, NAD+.

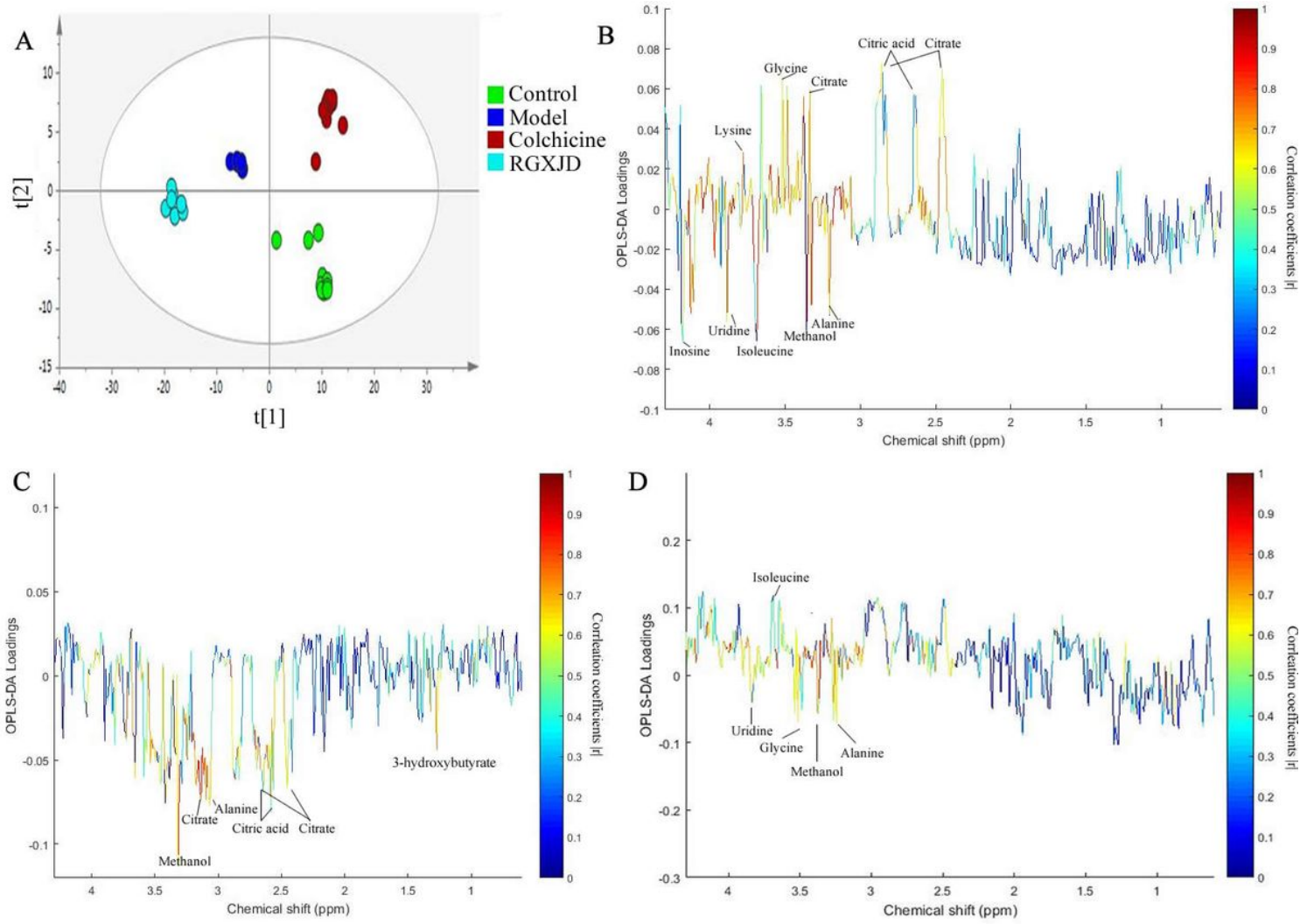

Figure 5

OPLS-DA score plot (A) and loading plot derived from 1H-NMR spectra of serum extracts (B-D) of all groups. B: Loading plot of rats serum between control and model group; C: Loading plot of rats serum between cohcile and model group; D: Loading plot of rats serum between RGXJD and model group.

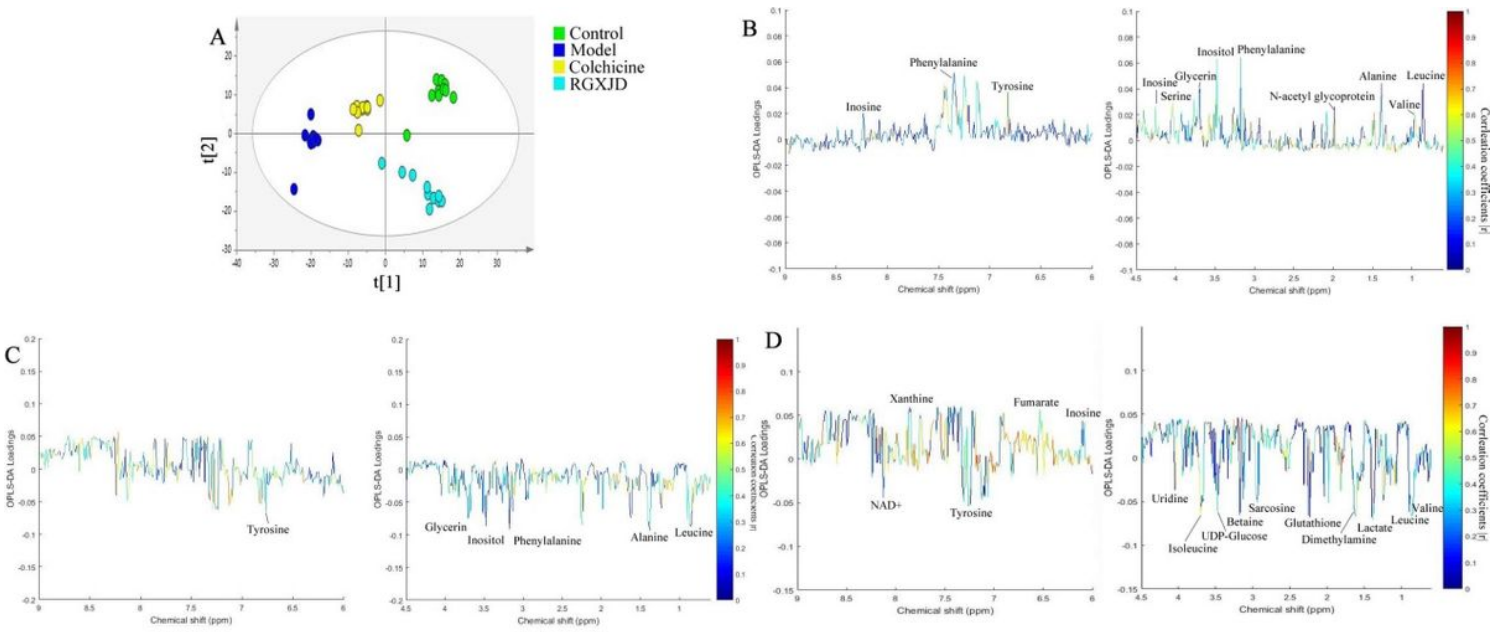

Figure 6

OPLS-DA score plot (A) and loading plot derived from 1H-NMR spectra of liver tissue extracts (B-D) of all groups. B: Loading plot of rats serum between control and model group; C: Loading plot of rats serum between cohcile and model group; D: Loading plot of rats serum between RGXJD and model group.

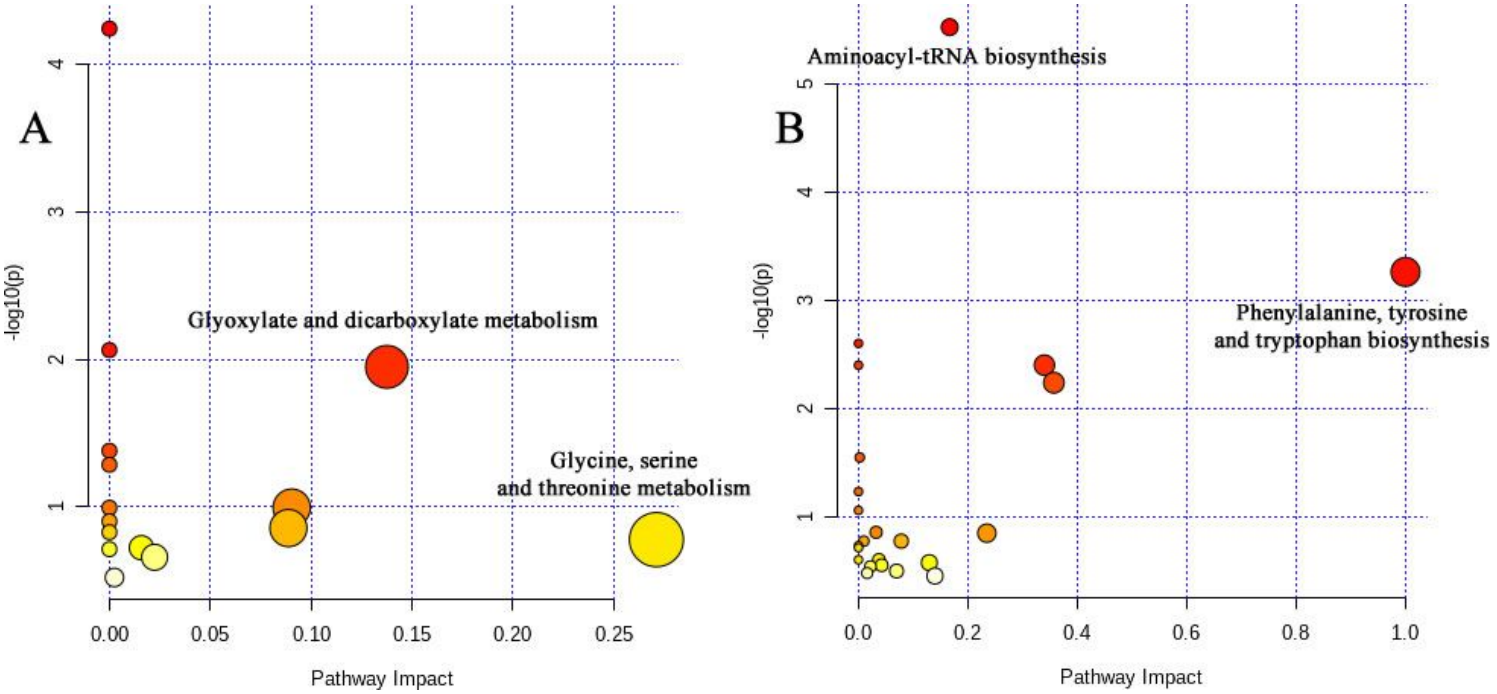

Figure 7

Summary of pathway analysis with MetaboAnalyst 4.0. Each point represents one metabolic pathway; the size of dot and shades of color are positive correlation with the impaction of metabolic pathway. (A. metabolism pathway involved in serum; B. metabolism pathway involved in liver)

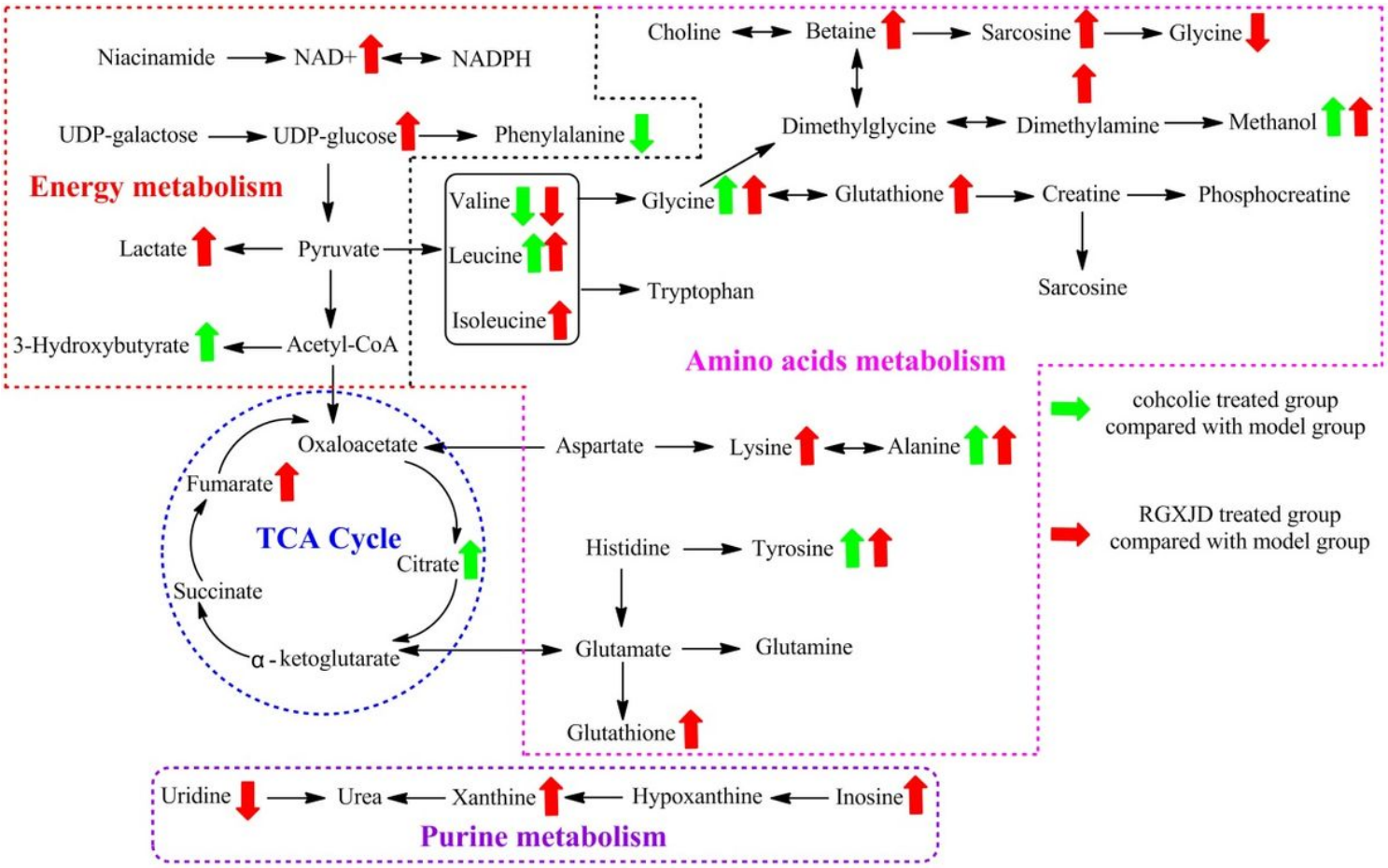

Figure 8

The main metabolic pathways in response to CCl4 induced liver fibrosis and the treatment effects of cohcolie and RGXJD, showing the interrelationship of the identified metabolic pathways. Arrows (“↑↓”) in different formats represented the notable increase or decrease of metabolites.

Supplementary Files

This is a list of supplementary files associated with this preprint. Click to download.

- SupplementaryMaterial0929.docx